Journal of Hydroscience and Hydraulic Engineering
Vol. 18, No.1 May, 2000, 53-60

# MICROSCOPIC AND MACROSCOPIC DISPERSIONS IN NUMERICALLY GENERATED HETEROGENEOUS POROUS MEDIA

By

Kei NAKAGAWA

Kyushu University, 6-10-1, Hakozaki, Higashi-Ku, Fukuoka, 812-8581, Japan

Kenji JINNO

Kyushu University, 6-10-1, Hakozaki, Higashi-Ku, Fukuoka, 812-8581, Japan

and

Tosao HOSOKAWA

Kyushu Sangyo University, 2-3-1, Matsukadai, Higashi-Ku, Fukuoka, 813-8503, Japan

## SYNOPSIS

An evaluation of the dispersion coefficient or the dispersivity is important for the solute transport in groundwater flow. In this paper, an evaluation of the dispersion coefficient by the numerical simulation for the heterogeneous porous media is attempted. The heterogeneous porous media consists of $39 \times 19$ blocks with the packed glass beads of six different diameters. For each block, microscopic dispersivity, hydraulic conductivity and porosity are known. The forty cases for evaluating the macroscopic dispersion are studied. Specifically, the relationship between the integral scale of the log-transformed hydraulic conductivity and macroscopic dispersivity is examined. It is suggested that the macroscopic dispersion depend on the integral scale and that the sufficiently large observation scale be necessary for obtaining the converged macroscopic dispersion coefficient.

## INTRODUCTION

In order to understand the flow and pollutant transport, it is important to know the characteristics of aquifer structure. Particularly, the determination of preferential path and the dispersion of contaminant plume is a crucial issue in groundwater pollutions (9). Kinzelbach (8), Appelo and Postma (1) discussed on the microscopic and macroscopic dispersions. Using the moment method, Tohma (16) made a theoretical and experimental study on the macroscopic dispersion coefficients in the stratified aquifer and in the aquifer where the hydraulic conductivity is modeled by the distribution function. Many approaches to the stochastic modeling of groundwater flow and dispersion have been made (e.g. (2), (3), (5), (6), (14), (15)). However, the studies on the relationship between the microscopic dispersion inherent in the aquifer material and the macroscopic one in the heterogeneous geological structure are limited.

In the present study, the numerical simulations are carried out to evaluate the macroscopic dispersion of the synthetically generated heterogeneous fields. Besides, key factors like integral length of the log-transformed hydraulic conductivity, macroscopic dispersivity, and observation scale are examined.

## METHOD OF EXAMINATION

Fig. 1 shows the flow chart of the present study. At first, the heterogeneous hydraulic conductivity field, which consists of the six different glass beads is synthetically generated. In order to characterize the generated fields, both the autocorrelation coefficient and spectrum distribution of log-transformed hydraulic conductivity are computed. The longitudinal integral scale of log-transformed hydraulic conductivity is determined from the autocorrelation coefficient.

In the numerical simulation, non-reactive tracer is injected at the vertical line source. The longitudinal direction is taken in the $x$-axis and the lateral direction is taken in the $y$-axis. The longitudinal dispersion coefficient is evaluated from the vertically averaged concentration distribution. Furthermore, the relationship between the macroscopic dispersivity and the longitudinal integral scale of log-transformed hydraulic conductivity is examined.

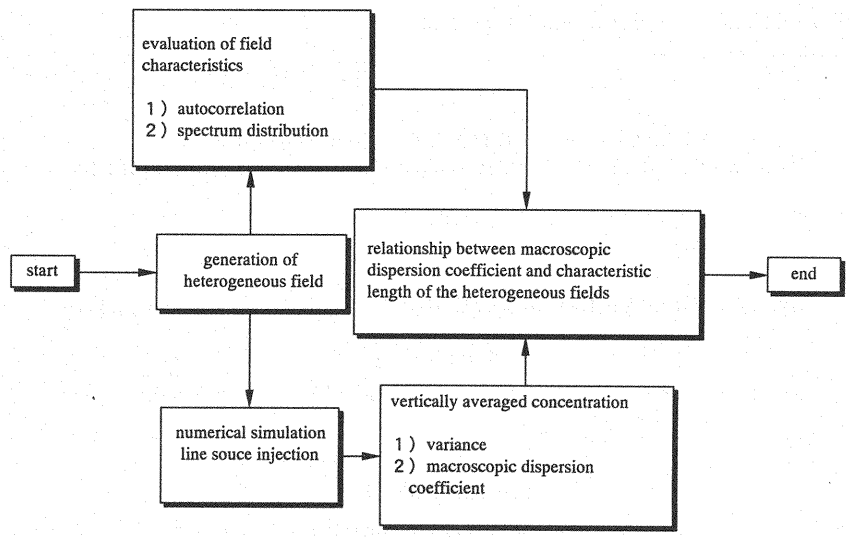


Fig. 1 Evaluation procedure of macroscopic dispersion

## GENERATION OF THE HETEROGENEOUS FIELD AND EVALUATION OF MACROSCOPIC DISPERSION

*Heterogeneous field*

Fig. 2 shows an example of heterogeneous field (*Run1*). The hydraulic conductivity, porosity, and longitudinal microscopic dispersivity for glass beads of different diameters are listed in Table. 1. The transverse microscopic dispersivity is taken one tenth of the longitudinal microscopic dispersivity (8). For the generation of heterogeneous fields, the assumption that the log-transformed hydraulic conductivity satisfies the auto-regressive model (Eq. 1) is employed (4), (13).

$$a_{xx}\frac{\partial^2 Y}{\partial x^2}+a_{yy}\frac{\partial^2 Y}{\partial y^2}-a_0 Y+\varepsilon(x,y)=0 \tag{1}$$

where $a_{xx}$, $a_{yy}$, and $a_0$ are the auto-regressive coefficients, $Y$ is the log-transformed hydraulic conductivity, and $\varepsilon(x, y)$ is the Gaussian white noise. After solving Eq. 1 by the finite difference method under the appropriate boundary conditions, the $Y$-value was assigned to six different classes as used in the previous study (12). In the present simulation (*Run1*), the values of the coefficients $a_{xx}$, $a_{yy}$ and $a_0$ were $a_{xx}=a_{yy}=25$ cm$^2$, $a_0=1$ and the variance of $\varepsilon$ was taken 1.5.

*Characteristics of the field*

In order to know the spatial characteristics of the fields, the spectrum distribution and autocrrelation coefficient were estimated. The spectrum distribution was computed by the Fast Fourier Transform (FFT). Fig. 3 shows the spectrum distribution of *Run1*. In this figure, $m$ and $n$ are the wave numbers in the $x$ and $y$ directions. It can be said that the field consists of a few wave components. The autocorrelation coefficient is defined by,

$$R(\xi,\eta)=\frac{\mathrm{E}\left[\left(Y(x,y)-\bar{Y}\right)\left(Y(x+\xi,y+\eta)-\bar{Y}\right)\right]}{\mathrm{E}\left[\left(Y(x,y)-\bar{Y}\right)^2\right]} \tag{2}$$

where $x$ and $y$ are the coordinates, $\xi$ and $\eta$ are the distance separation in the $x$ and $y$ directions, E[ ] is the expectation, and $\bar{Y}$ is the mean value of $Y$(=E[$Y(x, y)$]). $R(\xi, \eta)$ can be approximated by an exponential decay model (17) as,

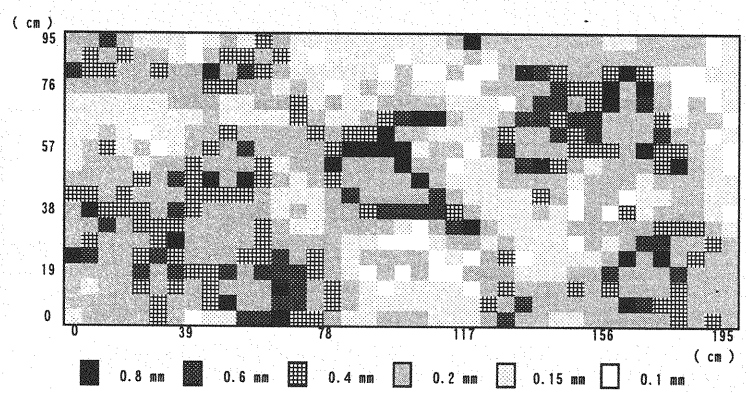


Fig. 2 Distribution of glass beads in generated heterogeneous field ( $a_{xx}=a_{yy}=25$ cm$^2$, $a_0=1$, $\sigma_\varepsilon^2=1.5$, and $L_x=L_y=5$ cm)

Table. 1 Hydraulic conductivity, porosity, and longitudinal microscopic dispersivity for glass beads of different diameters

| $d_m$ (mm) | $k$ (cm s$^{-1}$) | $n$ (%) | $\alpha_L$ (cm) |
|---|---|---|---|
| 0.1 | $8.92\times10^{-3}$ | 37.9 | $3.67\times10^{-3}$ |
| 0.15 | $1.84\times10^{-2}$ | 37.6 | $5.50\times10^{-3}$ |
| 0.2 | $2.98\times10^{-2}$ | 37.6 | $7.34\times10^{-3}$ |
| 0.4 | $8.57\times10^{-2}$ | 37.3 | $1.47\times10^{-2}$ |
| 0.6 | $2.16\times10^{-1}$ | 37.3 | $2.20\times10^{-2}$ |
| 0.8 | $3.58\times10^{-1}$ | 37.3 | $2.93\times10^{-2}$ |

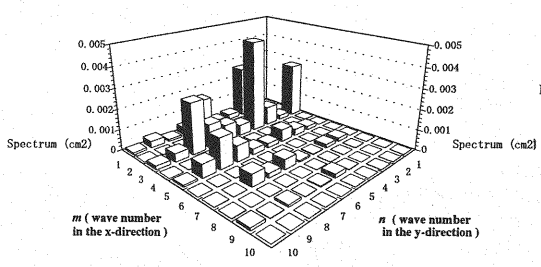


Fig. 3 Spectrum distribution

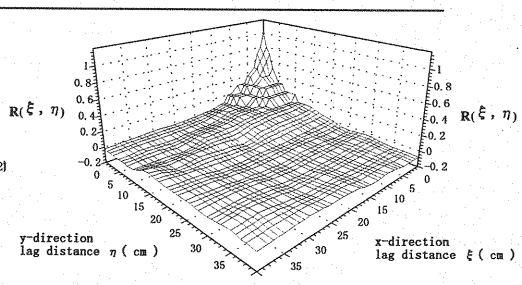


Fig. 4 Autocorrelation coefficient

$$R(\xi,\eta)=\exp\left[-\left(\left(\frac{\xi}{L_x}\right)^2+\left(\frac{\eta}{L_y}\right)^2\right)^{1/2}\right] \tag{3}$$

and when $\xi=0$ or $\eta=0$

$$R(\xi,0)=\exp\left[-\frac{|\xi|}{L_x}\right],\quad R(0,\eta)=\exp\left[-\frac{|\eta|}{L_y}\right] \tag{4}$$

where $L_x$ and $L_y$ are the integral scales of $Y$ in the $x$ and $y$ directions. Fig. 4 shows the autocorrelation coefficients for *Run1* and Fig. 5 shows for different $L_x$ and $L_y$. From the figure, it can be seen that the correlations approach zero at separations larger than 20 cm in both the $x$ and $y$ directions. The best fits for the simulated values are obtained when $L_x$ and $L_y$ are both equals to 5 cm.

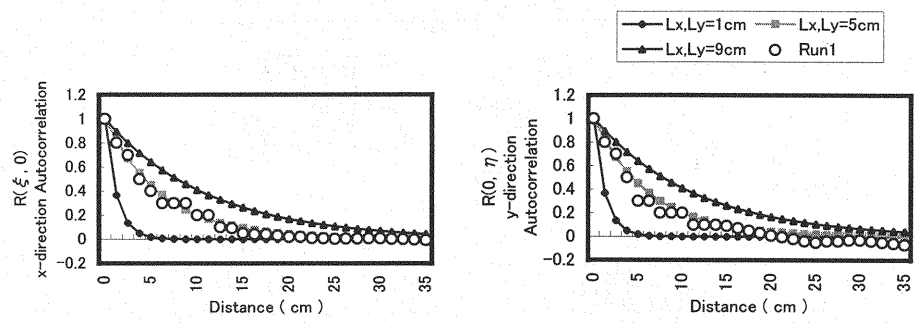


Fig. 5 Autocorrelation coefficients in $x$ and $y$ directions

*Numerical simulation*

In the numerical simulation, the equations of groundwater flow and non-reactive solute transport are applied. The effect of fluid density on the groundwater flow is considered because of the influence of NaCl as a tracer, and the density term is therefore included in the flow equation.

$$S_S \frac{\partial h}{\partial t} = \frac{\partial}{\partial x}\left[k\frac{\partial h}{\partial x}\right] + \frac{\partial}{\partial y}\left[k\left(\frac{\partial h}{\partial y} + \frac{\rho}{\rho_f}\right)\right] \tag{5}$$

$$\frac{\partial C}{\partial t} + \frac{\partial (u'C)}{\partial x} + \frac{\partial (v'C)}{\partial y} = \frac{\partial}{\partial x}\left(D_{xx}\frac{\partial C}{\partial x} + D_{xy}\frac{\partial C}{\partial y}\right) + \frac{\partial}{\partial y}\left(D_{yy}\frac{\partial C}{\partial y} + D_{yx}\frac{\partial C}{\partial x}\right) \tag{6}$$

where $S_s$ is the specific storage coefficient ($L^3L^{-3}$), $k$ is the hydraulic conductivity ($LT^{-1}$), $h$ is the pressure head (L), $u'$ and $v'$ are the pore velocities ($LT^{-1}$), $\rho$ is the density distribution ($ML^{-3}$), C(=( $\rho$ - $\rho_f$)/( $\rho_s$ - $\rho_f$)) is the normalized salt concentration (%), $\rho_f$ and $\rho_s$ are fresh and salt water densities ($ML^{-3}$).
The microscopic dispersion coefficients are defined as follows (7).

$$D_{xx} = \frac{\alpha_L u'}{V} + \frac{\alpha_T v'}{V} + \tau D_M, \quad D_{yy} = \frac{\alpha_T u'}{V} + \frac{\alpha_L v'}{V} + \tau D_M, \quad D_{xy} = D_{yx} = \frac{(\alpha_L - \alpha_T)u'v'}{V} \tag{7}$$

where $V=(u'^2+v'^2)^{1/2}$, $\alpha_L$: longitudinal microscopic dispersivity (L), $\alpha_T$: transverse microscopic dispersivity (L), $D_M$: molecular diffusion coefficient ($L^2T^{-1}$), $\tau$ :tortuosity.

A combined implicit finite difference and Gauss-Seidel method is employed to solve Eq. 5 (the groundwater flow equation). The method of characteristics (MOC) is used for solving Eq. 6 (11).

The upstream and downstream boundaries are the hydrostatic pressure boundaries. The top and bottom of the model aquifer are impermeable boundaries. The difference between the upstream and downstream pressure heads is maintained 50.5 cm. The simulation area is 195 cm in the $x$ direction and 95 cm in the $y$ direction. The grid intervals of $x$ and $y$ directions are taken 1.25 cm. The non-reactive tracer is introduced in the line at 26.25 cm apart from the upstream boundary of the model aquifer, because the plume may disperse toward the upstream. Fig. 6 shows the plume of *Run1* obtained from the numerical simulation for an instantaneous line injection of tracer. Microscopic dispersion occurs locally, and the macroscopic one can be observed for the vertically averaged concentration. At 1000 seconds after injection, the separation between faster and slower tracer transport portions becomes remarkable. Thus, the macroscopic dispersion in the $x$ direction is enlarged. The main flow of tracer is dominated in the high permeable zone composed of the glass beads of 0.8 mm and 0.6 mm in diameter. While, even after 3000 seconds the tracer has not arrived yet at the height from 65 cm to 95 cm of model aquifer. In the theory of a homogeneous field, the tracer is represented by Gaussian distribution for the vertically averaged concentration. In this case, however, the vertically averaged concentration has a few peaks and reveals the effect of heterogeneous dispersion.

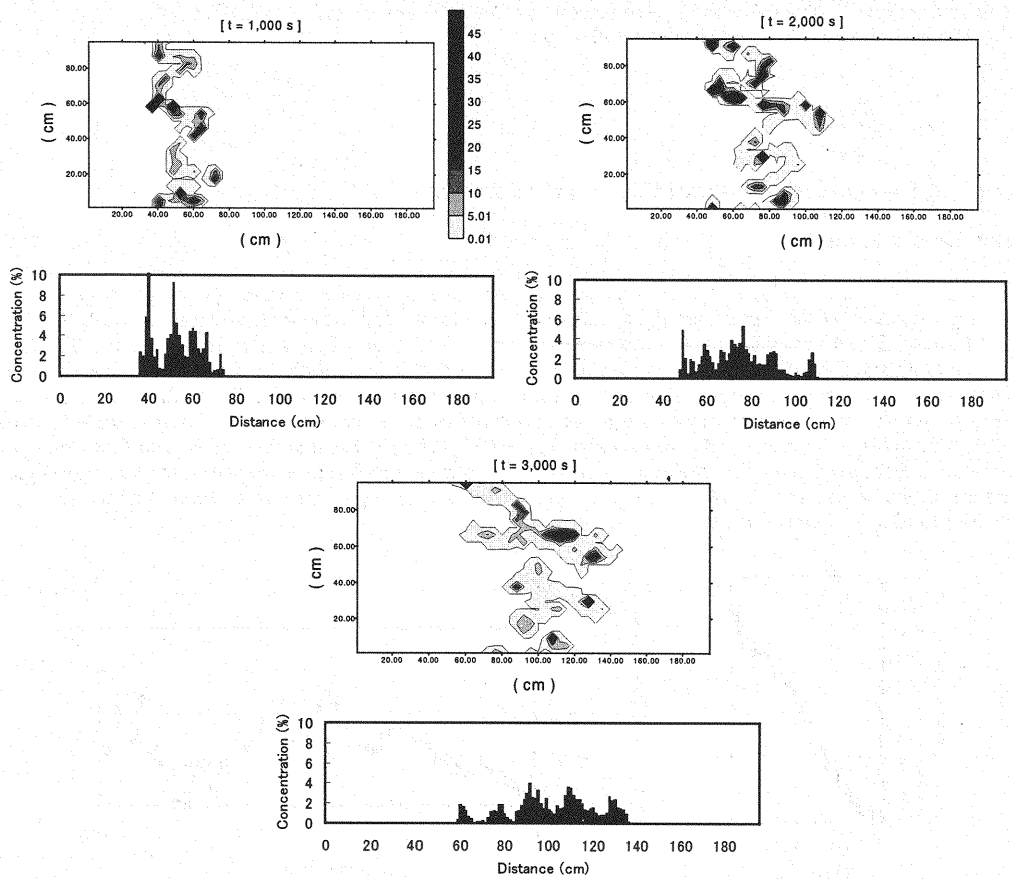


Fig. 6 Tracer movements and averaged concentration distributions from 1000 to 3000 seconds

*Evaluation of variance and macroscopic dispersion*

The time dependent variance in the $x$ direction is calculated by,

$$\sigma_L^2(t) = \frac{\sum C(x,t)(x-\bar{x})^2 \Delta x}{\sum C(x,t)\Delta x} \tag{8}$$

where $\bar{x}$ is the center of the vertically averaged concentration (10).

The macroscopic dispersion coefficient (10) is defined as,

$$D_L(t) = \frac{1}{2}\frac{d\sigma_L^2(t)}{dt} \tag{9}$$

Generally, the variance in a homogeneous field increases with travel time as a quadratic function of time at the early stage and as a linear function at the final stage. However, the variance oscillated irregularly for each realization in this case. The plume width increased in the high permeable zone and decreased in the low one alternately. The phenomena is shown in Fig. 7. The ensemble average over 10 realizations was calculated and the result is shown in Fig. 8. Although the transition period exists, $D_L$(t) tends to converge to 0.12 $cm^2s^{-1}$ after 1500 seconds. The characteristic time $T_{min}$ is defined as the intersection of the two lines as shown in Fig. 8. The change in $D_L$(t) can be classified into the two stages approximated by the two lines as

shown in the figure. The value of $T_{min}$ was estimated to be 600 seconds and $D_L$ = 0.12 $cm^2s^{-1}$.

The macroscopic dispersivity can be defined as,

$$A_L = \frac{D_L}{\bar{U}_{mean}} \tag{10}$$

where $\bar{U}_{mean}$ is the ensemble average of $U_{mean}$ over 10 realizations.

*Results and discussions*

Fig. 9a shows the relationship between the integral scale $L_x$ and the macroscopic dispersivity $A_L$. By changing the values of the parameters $a_{xx}$, $a_{yy}$, and $a_0$, $A_L$ can be related to the integral length $L_x$ as $A_L$=0.929× $L_x$. Similarly, Fig. 9b shows the relationships between $L_x$ and $T_{min}$, and $L_x$ and $X_{min}$, respectively. The value of $X_{min}$ was obtained by the procedure similar to $T_{min}$ shown in Fig. 8. Both $T_{min}$ and $X_{min}$ increase with the integral scale $L_x$ as shown in Figs. 9a and 9b. According to the relation of $X_{min}$=3.37×$L_x$, the macroscopic dispersion coefficient or dispersivity converges after a distance of several times of the integral scale $L_x$ in the present simulation. Therefore, the parameters $T_{min}$ or $X_{min}$ should be simultaneously clarified when the macroscopic dispersion process is defined. In practice, however, detailed information on the hydrogeological structure of aquifer is limited. More practical approaches, for example, the use of vertical tracer profile in boreholes need to be developed.

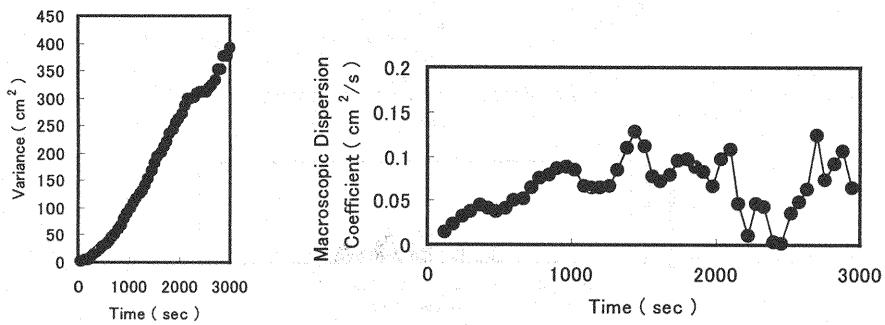


Fig. 7 Variance and macroscopic dispersion coefficient of vertically averaged concentration

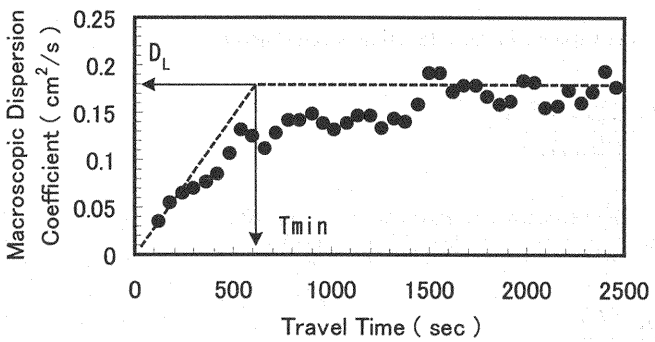


Fig. 8 The ensemble average of the macroscopic dispersion coefficient as a function of travel time ($L_x$=5 cm)

## CONCLUSIONS

In this study, macroscopic dispersion in heterogeneous porous media was examined by the numerical simulation. The following conclusions can be drawn from the present study :

1) The relationship between integral scale of log-transformed hydraulic conductivity and macroscopic dispersivity (or macroscopic dispersion coefficient) is almost linear.

2) If the tracer is transported downstream about 3.4 times of the integral scale, macroscopic dispersivity and macroscopic dispersion coefficient is almost a constant value.

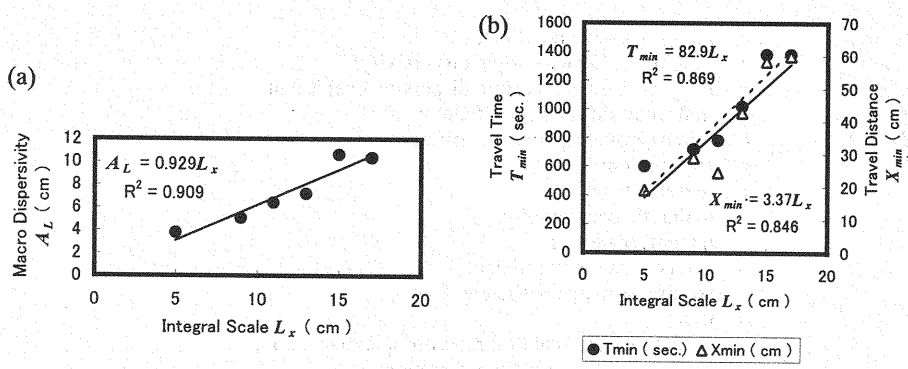


Fig. 9 (a) The relationship between the integral scale and the macroscopic dispersivity, and (b) the relationship between the integral scale, and travel time or travel distance

## REFERENCES


1. Appelo, C.A.J. and D. Postma : Geochemistry, Groundwater and Pollution, A.A.Balkema, Rotterdam, The Netherlands, 1994.
2. Dagan, G. : Stochastic modeling of groundwater flow by unconditional and conditional probabilities 2.The solute Transport, Water Resources Research, Vol.18, No.4, pp.835-848, 1982.
3. Dagan, G. : Transport in heterogeneous porous formations, ergodicity and effective dispersion, Water Resources Research, Vol.26, No.6, pp.1281-1290, 1990.
4. Elfeki, A.M.M., G.J.M. Uffink and F.B.J. Barends : Groundwater Contaminant Transport Impact of Heterogeneous Characterization, A.A.Balkema, Rotterdam, The Netherlands, 1997.
5. Gelhar, L.W. and C.L. Axness : Three-dimensional stochastic analysis of macrodispersion in aquifers, Water Resources Research, Vol.19, No.2, pp.161-180, 1983.
6. Gelhar, L.W. : Stochastic subsurface hydrology from theory to applications, Water Resources Research, Vol.22, No.9, pp.135S-145S, 1986.
7. Huyakorn, P.S. and G.F. Pinder : Computational Method in Subsurface Flow, Academic Press, New York, USA, 1983.
8. Kinzelbach, W. : Groundwater Modeling An Introduction with Sample Programs in Basic, Elsevier, Amsterdam, The Netherlands, 1986.
9. Tompson, A.F.B. and K.J. Jackson : Reactive transport in heterogeneous systems : an overview, Reactive Transport in Porous Media, Lichter, P.C., C.I. Steefel, and E.O. Oelkers ed., Reviews in Mineralogy, Vol.34, Mineralogical Society of America, pp.269-310, 1996.
10. Momii, K., K. Jinno, and T. Ueda : Effects of viscous sublayer on convective dispersion by numerical study, Proceedings of the 27th Japanese Conference on Hydraulics, pp.609-614, 1983 (in Japanese).
11. Momii, K. : Applications of the finite difference method and method of characteristics to solute transport analysis, Journal of Groundwater Hydrology, Vol.33, No.3, 177-184, 1991 (in Japanese).
12. Nakagawa, K., K. Jinno, T. Hosokawa, K. Hatanaka, Y. Ijiri, and S. Watari : Groundwater flow and mass transport in a non-uniform porous medium, Journal of Groundwater Hydrology, Vol.40, No.1, pp.1-16, 1998 (in Japanese).
13. Smith, L. and R.A. Freeze : Stochastic analysis of steady state groundwater flow in a bounded domain, 2.Two-dimensional Simulations, Water Resources Reserch, Vol.15, No.6, pp.1543-1559, 1979.
14. Smith, L. and F.W. Schwartz : Mass transport 1. A stochastic analysis of macroscopic dispersion, Water Resources Research, Vol.16, No.2, pp.303-313, 1980.
15. Sudicky, E.A. : A natural gradient experiment on solute transport in a sand aquifer, spatial variability of hydraulic conductivity and its role in the dispersion process, Water Resources Research, Vol.22, No.13, pp.2069-2082, 1986.
16. Tohma, S. : A Fundamental Study on The Estimation of Parameters for Groundwater Flow, Doctor Thesis, Kyushu University, 1989 (in Japanese).
17. Ueda, T., K. Jinno, and F. Hirano : Estimation of transmissivity and unsteady groundwater level in muromi river basin, Proceedings of the 28th Japanese Conference on Hydraulics, pp.601-608, 1984 (in Japanese).

## APPENDIX-NOTATION

The following symbols are used in this paper:

| | | |
|---|---|---|
| $a_{xx}, a_{yy}, a_0$ | = | auto-regressive coefficient; |
| $A_L$ | = | longitudinal macroscopic dispersivity; |
| $D_L$ | = | longitudinal macroscopic dispersion coefficient; |
| $D_M$ | = | molecular diffusion coefficient; |
| $D_{xx}, D_{yy}, D_{xy}, D_{yx}$ | = | microscopic dispersion coefficient; |
| E[ ] | = | expectation; |
| $h$ | = | pressure head; |
| $k$ | = | hydraulic conductivity; |
| $L_x, L_y$ | = | integral scale of $Y$; |
| $R$ | = | autocorrelation coefficient; |
| $S_s$ | = | specific storage coefficient; |
| $t$ | = | time; |
| $T_{min}$ | = | minimum time scale for macroscopic dispersion; |
| $\underline{U}_{mean}$ | = | averaged velocity in the $x$ direction; |
| $U_{mean}$ | = | ensemble average of $U_{mean}$; |
| $\underline{u}', v'$ | = | pore velocity; |
| $\bar{x}$ | = | center of the vertically averaged concentration; |
| $X_{min}$ | = | minimum spatial scale for macroscopic dispersion; |
| $x, y$ | = | coordinates; |
| $Y$ | = | log-transformed hydraulic conductivity; |
| $\alpha_L, \alpha_T$ | = | longitudinal and transverse microscopic dispersivity; |
| $\varepsilon$ | = | Gaussian white noise; |
| $\rho$ | = | density; |
| $\xi, \eta$ | = | distance separation; |
| $\sigma_L^2$ | = | variance of vertical averaged concentration in the $x$ direction; and |
| $\tau$ | = | tortuosity. |

(Received August 2, 1998 ; revised March 18, 2000)